ANTIMICROBIAL AGENTS AND CHEMOTHERAPY, Sept. 2006, p. 3124–3131 Vol. 50, No. 9
0066-4804/06/$08.00+0 doi:10.1128/AAC.00394-06

Tetracyclines Specifically Target the Apicoplast of the Malaria Parasite *Plasmodium falciparum*

Erica L. Dahl,[1] Jennifer L. Shock,[2] Bhaskar R. Shenai,[1]† Jiri Gut,[1] Joseph L. DeRisi,[2] and Philip J. Rosenthal[1]*

Department of Medicine, Box 0811,[1] and Department of Biochemistry and Biophysics, Box 2240,[2] University of California—San Francisco, San Francisco, California 94143

Received 30 March 2006/Returned for modification 2 June 2006/Accepted 13 June 2006

Tetracyclines are effective but slow-acting antimalarial drugs whose mechanism of action remains uncertain. To characterize the antimalarial mechanism of tetracyclines, we evaluated their stage-specific activities, impacts on parasite transcription, and effects on two predicted organelle targets, the apicoplast and the mitochondrion, in cultured *Plasmodium falciparum*. Antimalarial effects were much greater after two 48-h life cycles than after one cycle, even if the drugs were removed at the end of the first cycle. Doxycycline-treated parasites appeared morphologically normal until late in the second cycle of treatment but failed to develop into merozoites. Doxycycline specifically impaired the expression of apicoplast genes. Apicoplast morphology initially appeared normal in the presence of doxycycline. However, apicoplasts were abnormal in the progeny of doxycycline-treated parasites, as evidenced by a block in apicoplast genome replication, a lack of processing of an apicoplast-targeted protein, and failure to elongate and segregate during schizogeny. Replication of the nuclear and mitochondrial genomes and mitochondrial morphology appeared normal. Our results demonstrate that tetracyclines specifically block expression of the apicoplast genome, resulting in the distribution of nonfunctional apicoplasts into daughter merozoites. The loss of apicoplast function in the progeny of treated parasites leads to a slow but potent antimalarial effect.

Plasmodium falciparum causes an estimated half billion cases of malaria, resulting in over a million deaths, each year (5, 33). Tetracyclines are effective, albeit slow-acting, antimalarials that are used in combination with a more rapidly acting drug to treat malaria (1) and for antimalarial chemoprophylaxis (29). The antimalarial mechanism of action of tetracyclines remains undefined. Consistent with their slow clinical activity, tetracyclines exert in vitro antimalarial effects slowly, requiring incubation with cultured *P. falciparum* beyond a single 48-h asexual cycle for maximal effects (16). Tetracyclines exert antibacterial activity by inhibiting prokaryotic translation (41). However, in the eukaryote *P. falciparum*, protein synthesis is broadly inhibited by tetracyclines only at much higher concentrations than those required to block parasite growth (6), suggesting that their antimalarial effects are due to action against a target other than cytosolic ribosomes.

Early studies of the mechanism of action of tetracyclines against *P. falciparum* focused on the parasite's single mitochondrion as the likely target (18, 26). However, these studies preceded the identification of the apicoplast, an organelle of uncertain function that is related to the chloroplast of plant cells (20, 42). The mitochondrion and the apicoplast each contain their own genome, encoding prokaryote-like ribosomal RNAs, tRNAs, and some proteins (12, 45). In addition, several hundred nuclear genes encode proteins targeted to the apicoplast or the mitochondrion (2, 14, 15, 28, 39). The apicoplast houses enzymes involved in type II fatty acid synthesis, a nonmevalonate pathway for isoprenoid biosynthesis, and heme-biosynthetic pathways (44). The mitochondrion maintains a mitochondrial membrane potential and houses a complete citric acid cycle. However, its role in energy generation is still unclear, since a link from the citric acid cycle to the electron transport chain remains to be defined (36). The mitochondrion does house a number of enzymes involved in pyrimidine and heme biosynthesis, and disruption of either organelle would be expected to block critical biosynthetic pathways. Since both organelles contain prokaryote-like ribosomal components, either is a potential target of tetracyclines.

To better characterize the antimalarial mechanism(s) of tetracyclines, we evaluated their activities over two 48-h parasite life cycles. We then evaluated the effects of doxycycline on parasite gene expression by microarray analysis and on specific mitochondrion and apicoplast self-maintenance functions. Our results are consistent with a model in which doxycycline specifically inhibits the production of proteins encoded by the apicoplast genome, leading to a subsequent loss of apicoplast function and a delayed but potent antimalarial effect.

MATERIALS AND METHODS

Malaria parasites and culture. *P. falciparum* parasites were cultured in human erythrocytes maintained at 2% hematocrit in RPMI 1640 medium with 0.5% (wt/vol) AlbuMAX II (Invitrogen-Gibco) in 92% N_2, 5% CO_2, and 3% O_2 (35). Synchrony was maintained by serial sorbitol treatments (21). Strain W2 was used for the determination of 50% inhibitory concentrations (IC_{50}s) and microscopy, and 3D7 was used in microarray and Southern analyses. Parasites stably expressing green fluorescent protein fused to an acyl carrier protein apicoplast-targeting sequence (ACP_I-GFP), kindly provided by Geoff McFadden (40), were maintained in medium containing 100 nM pyrimethamine. Dually transfected parasites stably expressing a red fluorescent protein fused to an acyl carrier protein apicoplast-targeting signal and a yellow fluorescent protein fused to a citrate

* Corresponding author. Mailing address: Box 0811, Department of Medicine, University of California, San Francisco, CA 94143-0811. Phone: (415) 206-8845. Fax: (415) 648-8425. E-mail: rosnthl@itsa.ucsf.edu.

† Present address: Metagenics, Inc., 9770 44th Ave. NW, Suite 100, Gig Harbor, WA 98332.

synthetase mitochondrial targeting signal (ACP_L-DsRed and CS_L-YFP), also kindly provided by Geoff McFadden (37), were maintained in medium containing 5 nM WR99210.

Unless stated otherwise, all doxycycline studies were carried out as follows. Synchronized parasites were treated at the late ring/early trophozoite stage (approximately 20 h postinvasion) with 1 μM doxycycline or an equivalent volume of dimethyl sulfoxide (DMSO) for 24 h, until they reached the late schizont stage. The parasites were then subcultured into fresh medium and allowed to invade new erythrocytes and progress through a second cycle in the absence of drug. The medium was replaced every 24 h. Doxycycline, minocycline, tetracycline, and pyrimethamine were from Sigma. WR99210 was the gift of David Jacobus (Jacobus Pharmaceuticals).

Antiparasitic effects of tetracyclines. W2 strain parasites were cultured in 96-well plates at initial parasitemias of 1% for 48-h and 0.2% for 96-h drug studies. Serial dilutions of tetracyclines (100 μM to 1 nM; dissolved in DMSO) and chloroquine (dissolved in water) were prepared in complete medium. Equivalent volumes of DMSO were included as controls.

The IC_{50} of each drug was determined by comparing parasite counts by flow cytometry and the uptake of [^{3}H]hypoxanthine by standard methods. For flow cytometry, after incubation with the drugs, infected erythrocytes were fixed in 1% paraformaldehyde in phosphate-buffered saline (PBS) for 48 h, permeabilized with 0.1% Triton X-100, and stained with 1 nM YOYO-1 (Molecular Probes). Parasitemias were determined from dot plots (forward scatter versus fluorescence) acquired on a FACSort cytometer using CELLQUEST software (Becton Dickinson). Hypoxanthine uptake assays were performed essentially as described previously (8). Briefly, late-ring-stage-infected erythrocytes were cultured in medium containing 10 μCi/ml [^{3}H]hypoxanthine (NEN Life Sciences) for 48 h and then harvested and washed using a PHD Cell Harvester (Cambridge Technology Inc.). ^{3}H incorporation was assessed in a Beckman LS 6000IC scintillation counter (Beckman Coulter Inc.). IC_{50}s were calculated from variable-slope sigmoidal dose-response curves using GraphPad Prism version 3.00 for Windows (GraphPad Software).

Microscopy. For light microscopy, thin smears were prepared, stained with Giemsa stain, and photographed using a SPOT Flex Color Mosaic Digital Camera (Diagnostic Instruments) on a Nikon Optiphot microscope. For electron microscopy, infected erythrocytes were washed in PBS, fixed in Karnovsky's solution (1% paraformaldehyde, 3% glutaraldehyde, 0.1 M sodium cacodylate buffer, pH 7.4) for 4 h at room temperature, and then stored at 4°C until they were analyzed. Fixed samples were postfixed in reduced OsO_4 (2% OsO_4 plus 1.5% potassium ferrocyanide; Sigma) and stained en bloc with uranyl acetate before being dehydrated in ethanol, cleared in propylene oxide, and embedded in Eponate 12 (Ted Pella Co). Thin sections were cut with a Leica ultracut UCT microtome, stained with uranyl acetate and Reynold's lead, and examined with a Philips Tecnai 10 electron microscope. Photographs were scanned using a CanoScan N6700 (Canon).

For fluorescence microscopy of ACP_L-GFP parasites, infected erythrocytes were fixed in 1% formaldehyde, 0.1% gluteraldehyde, and a 1:400 dilution of DAPI (4′,6′-diamidino-2-phenylindole) nuclear stain (Molecular Probes) in PBS; pipetted onto poly-L-lysine-coated microscope slides; incubated for 30 min at room temperature; washed in PBS; air dried; and overlaid with mounting solution (10% Mowiol 4-88, 25% glycerol, 2.5% 1,4-diazobicyclo-[2.2.2]-octane, 0.1 M Tris-HCl, pH 8.5) (17) and a coverslip. For fluorescence microscopy of live ACP_L-DsRed CS_L-YFP parasites, infected erythrocytes were rinsed in serum-free RPMI medium and allowed to attach to a poly-L-lysine-coated microscope slide for 30 min. The slides were then rinsed in serum-free RPMI medium, overlaid with a coverslip, and imaged immediately. Fluorescent images were captured using a SPOT Flex Color Mosaic Digital Camera (Diagnostic Instruments) on a Nikon Optiphot microscope. Merged images were assembled and optimized (background corrections and gamma adjustments) using SPOTsoftware version 4.5 (Diagnostic Instruments). For all microscopy, final figures were prepared in Adobe Photoshop version 5.5.

Microarray analysis. Parasites were incubated with doxycycline for 20 h and then subcultured and maintained in drug-free medium for an additional 35 h. Infected erythrocytes were collected every 5 h, lysed with 0.1% saponin for 5 min, centrifuged at 12,000 × *g* at 4°C, flash frozen in an ethanol-dry ice bath, and stored at −80°C. Total parasite RNA was harvested using TRIzol reagent (Invitrogen). For each sample, 12 μg of total parasite RNA was reverse transcribed into cDNA containing amino-allyl-dUTP (Ambion) using SuperScript II RNase H-Reverse Transcriptase (Invitrogen) and then coupled to succidimyl ester Cy5 dye (Amersham) as described previously (4). Cy5-labeled sample cDNA and a reference pool of Cy3-labeled cDNA representing all life cycle stages were competitively hybridized to a *P. falciparum* 70-mer microarray as described previously (3). The microarrays were scanned using a GenePix 4000B scanner, and images were analyzed using GenePix3 Software (Molecular Devices, Inc.), stored, and normalized using the NOMAD database (http://ucsf-nomad.sourceforge.net/). Expression data were log transformed and mean centered. Self-organizing map and cluster analysis was performed using Cluster software and visualized using Treeview (11).

TABLE 1. Antimalarial activities of tetracyclines[a]

Time of assay (h)	IC_{50} (μM)			
	Doxycycline	Minocycline	Tetracycline	Chloroquine
Parasite counts				
48	4.8 ± 0.2	4.6 ± 0.2	22.3 ± 0.5	0.10 ± 0.02
96	0.46 ± 0.07	0.14 ± 0.03	0.45 ± 0.01	0.083 ± 0.012
Hypoxanthine uptake				
48	16.0 ± 3.0	10.8 ± 1.3	51.0 ± 1.0	0.13 ± 0.03
96	1.02 ± 0.24	0.35 ± 0.08	1.27 ± 0.53	0.073 ± 0.006

[a] W2-strain parasites were incubated with drugs for 48 h, beginning at the late ring stage, and then analyzed or cultured for an additional 48 h in the absence of drugs before analysis. Ring stage parasitemias were determined by counting YOYO-1-stained infected erythrocytes by flow cytometry. Metabolic activity was assessed by quantitation of [^{3}H]hypoxanthine uptake. IC_{50}s are means ± standard errors of the mean from two independent experiments, each performed in duplicate.

Southern hybridization. Total DNA was isolated from schizont stage parasites using the Puregene DNA Purification kit (Gentra) and digested with XmnI and SacI, and samples (5 μg per lane) were electrophoresed on a 0.7% agarose gel and transferred to a Hybond N+ nylon membrane (Amersham Biosciences).

For probes, we amplified a 511-bp fragment of the mitochondrial genome between nucleotides 4998 and 5509 (which includes the putative ribosomal-DNA sequences *ssuD* and *lsuA* [12]) (primers, 5′ ACGCTGACTTCCTG 3′ and 5′ AGAAAACAGTCGGTG 3′) from genomic *P. falciparum* DNA, a 573-bp fragment of the apicoplast gene *tufA* (primers 5′ ATAGGAGCCACACA 3′ and 5′ TCCGGATTGTGCTT 3′) from genomic *P. falciparum* DNA, and a 500-bp fragment of the nuclear gene *falcipain-3* from the plasmid pTOPO-FP3 (31) (primers 5′ TACCATGGTACATAAGCTTCTGTTCCAATTGAACAA 3′ and 5′ TTAGAATTCTCATGTTGGGCTTTTAGTAGT 3′). Probes were gel purified and extracted using the QIAGEN Gel Extraction Kit and then labeled with [α-^{32}P]dATP using the Megaprime DNA Labeling System (Amersham Biosciences). Blots were prehybridized for 5 h in RapidHyb hybridization buffer (Amersham Biosciences) at 56°C and hybridized overnight at 65°C with the probes. The blots were then washed twice at 25°C in 2× SSC (SSC is 0.15 M NaCl/0.15 M Na citrate, pH 7.0), 0.1% sodium dodecyl sulfate (SDS); once at 55°C in 1× SSC, 0.1% SDS; and once at 60°C in 1× SSC, 0.1% SDS before visualization by autoradiography.

Immunoblots. ACP_L-GFP-containing parasites were isolated from erythrocytes with saponin, and denatured samples (5×10^7 parasites per lane) were electrophoresed on 12.5% polyacrylamide gels under reducing conditions. Proteins were transferred to polyvinylidene difluoride membranes and probed with mouse anti-GFP antibodies (Molecular Probes; 1:400), followed by alkaline phosphatase-conjugated donkey anti-mouse secondary antibody (Jackson ImmunoResearch Laboratories; 1:10,000) using standard procedures. Immunoblots were developed using the Western-*Star* Chemiluminescent Immunoblot Detection System with CDP-*Star* substrate (Applied Biosystems). The blots were stripped and reprobed with a 1:10,000 dilution of rat anti-falcipain-3 antibody (31), followed by alkaline phosphatase-conjugated goat anti-rat antibody (Jackson ImmunoResearch Laboratories; 1:10,000).

Nucleotide sequence accession numbers. All microarray data are available at the Gene Expression Omnibus database (http://www.ncbi.nlm.nih.gov/geo/), accession no. GSE5267.

RESULTS

Delayed antimalarial activities of tetracyclines. We evaluated the antimalarial activities of tetracycline, doxycycline, and minocycline over two 48-h parasite life cycles with standard assays, comparing either the uptake of hypoxanthine or the multiplication of parasites between treated and control para-

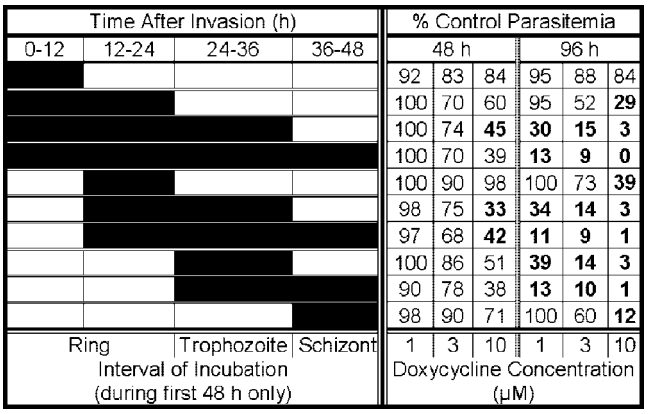

FIG. 1. Delayed effects of doxycycline are stage dependent. Highly synchronized parasites were treated with doxycycline for different intervals during a single life cycle, as indicated by the black shading. Parasitemias (% control) were determined 48 or 96 h after the start of the experiment. Note that inhibitory effects of doxycycline were much greater after two cycles (results with >50% inhibition are in boldface), even though the drug was removed after the first cycle.

sites. The concentrations of these antibiotics in human plasma after standard dosing ranges between 4.7 and 5.6 μM for tetracycline, 3.7 and 4.3 μM for doxycycline, and 5.0 and 7.7 μM for minocycline (34). When assessed based on activity during a single cycle, the tetracyclines were relatively inactive, with IC_{50}s above clinically relevant concentrations (Table 1). The tetracyclines showed much greater potency when assessed after a second cycle, consistent with earlier reports of slow action against malaria parasites (16, 25), with IC_{50}s at concentrations that are achievable with standard dosing of these agents. Remarkably, the increased potency after a second cycle was seen even if the tetracyclines were removed from culture after the first cycle of incubation (Table 1). Since doxycycline is the most widely used tetracycline to treat and prevent malaria, we chose it as our model compound for further characterizing the antimalarial actions of tetracyclines. To characterize stage-specific activity, we cultured parasites in doxycycline over different portions of the first cycle and evaluated the subsequent effects (Fig. 1). Trophozoite and early schizont stage parasites were most sensitive to doxycycline; incubations during the ring or late schizont stage had much less effect.

Doxycycline-treated parasites appeared to be morphologically normal through the entire first 48-h erythrocytic cycle (Fig. 2A), producing merozoites that invaded erythrocytes and formed normal-appearing daughter ring stage parasites. The parasites continued to develop through the second cycle and initiated schizogeny, with the appearance of multiple daughter nuclei. However, the mature schizonts became increasingly abnormal and failed to progress to merozoite release and subsequent erythrocyte invasion. Electron micrographs also showed that mature schizonts during the initial cycle of incubation with doxycycline (40 h) appeared to be normal. In the second cycle (88 h), doxycycline-treated schizonts lacked defined intracellular compartments, and many displayed abnormal vacuolation (Fig. 2B). The observed blocks in merozoite maturation and egress at 96 h were apparent even if drugs were removed after 48 h of incubation (not shown).

Expression of genes encoded by the apicoplast is specifically disrupted by doxycycline. To identify specific targets of doxycycline, we compared the transcriptomes of doxycycline-treated and control parasites over a 55-h period, beginning in early trophozoites (treatment began approximately 18 h postinvasion) through the mature trophozoite stage of the following cycle (approximately 24 h postinvasion). The patterns of

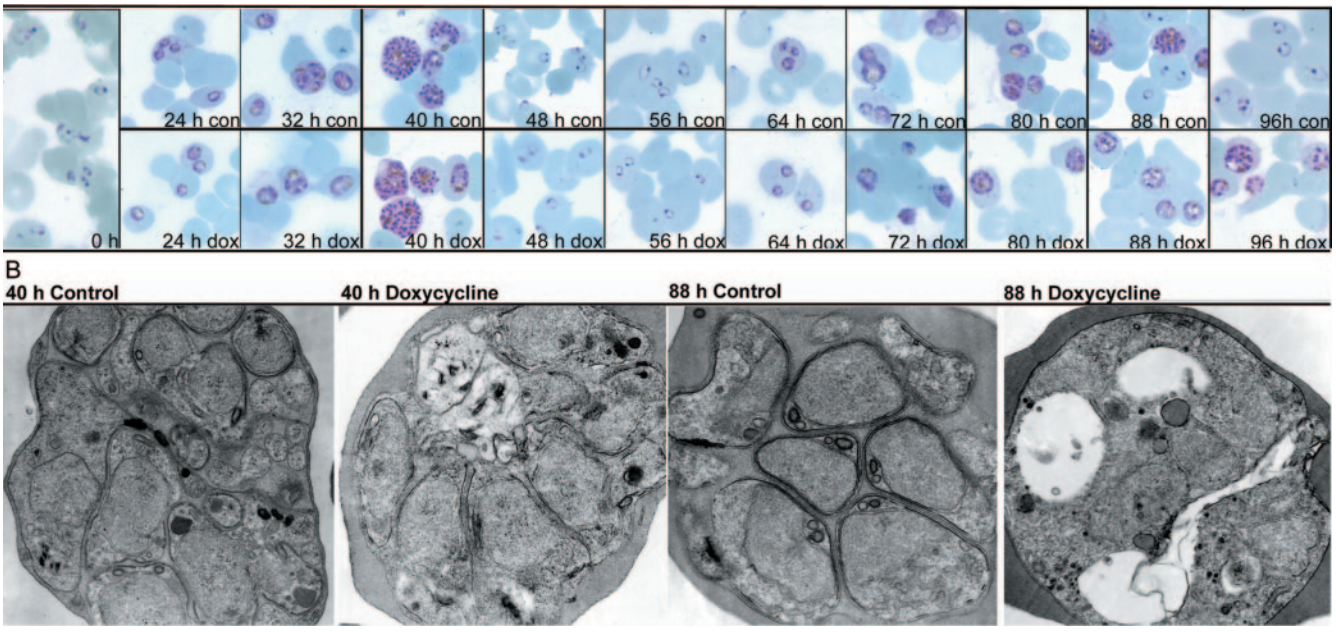

FIG. 2. Doxycycline causes morphological abnormalities late in the second cycle of treatment. Synchronized parasites were treated with 1 μM doxycycline or 0.1% DMSO (control) over two life cycles, beginning at the early ring stage (0 h). (A) Parasites were analyzed every 8 h by light microscopy of Giemsa-stained smears. (B) Parasites at 40 and 88 h were analyzed by electron microscopy.

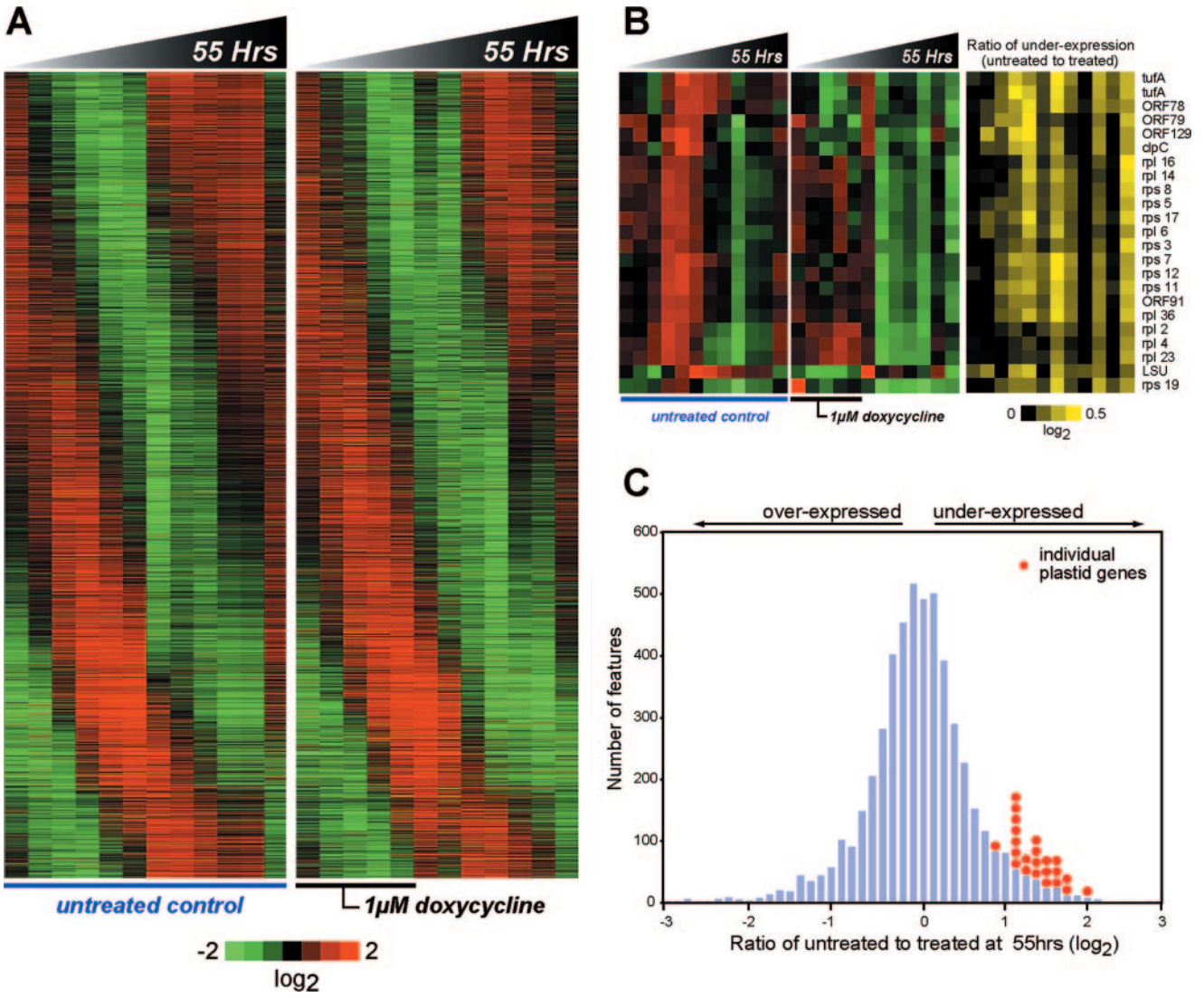

FIG. 3. Transcriptome analysis of doxycycline-treated parasites reveals lower mRNA abundance of apicoplast genes. Early trophozoites (approximately 20 h postinvasion) were treated with 1 μM doxycycline or 0.1% DMSO for 20 h and then transferred to drug-free media and cultured for an additional 35 h. RNA was isolated from samples collected every 5 h, converted into labeled cDNA, and hybridized to a 70-mer-based microarray as previously described (3). (A) Expression data from an overview set of 3,721 oligonucleotide features were plotted according to the phase of expression, derived from previous analysis (3). Increased expression is shown in red, and decreased expression in green. (B) For plastid genes, excluding tRNAs, the ratio of underexpresssion was plotted in yellow. (C) A histogram of the ratio between treated and untreated parasites at the final time point was plotted. The positions and numbers of plastid genes, excluding tRNAs, are shown as red dots.

gene expression in the doxycycline-treated and control parasites were remarkably similar (Fig. 3A). Using an overview gene set derived from a previously described intraerythrocytic developmental cycle transcriptome (3), we calculated the average correlation of expression profiles between treated and untreated cultures to be 0.80, indicating very little variation in gene expression following doxycycline treatment.

Subtle differences between microarray time courses can be detected by calculating the relative expression ratio between two samples at each time point (23, 24). We calculated the relative ratios between the untreated and treated time courses and then filtered the data set for array features (70-mers representing *P. falciparum* coding regions) representing genes that were consistently underexpressed in doxycycline-treated parasites, using modest criteria (greater than 1.6-fold underexpression at at least half of the time points). Only 104 array features (less than 2%) met these criteria. To assess whether any functional groups of genes were overrepresented in this set relative to the entire data set, we used the LACK software tool to calculate the statistical significance of lexical bias in the PlasmoDB annotations of our underexpressed gene set (19). The annotation "plastid" (signifying genes on the plastid genome), but no other annotation term, was significantly overrepresented ($P < 10^{-6}$, as calculated by binomial distribution) in our set of underexpressed genes. Indeed, essentially all of the plastid genes represented on our microarray were consistently underexpressed (Fig. 3B).

To assess the degree of underexpression relative to the dis-

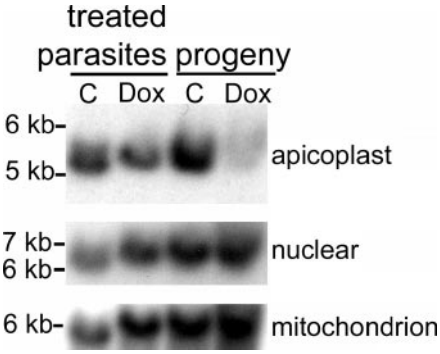

FIG. 4. Replication of the apicoplast genome was blocked in the progeny of doxycycline-treated parasites. Parasites were treated with 1 μM doxycycline (Dox) or 0.1% DMSO (C) for 24 h, beginning at the late ring stage, and then subcultured into fresh medium and allowed to continue a second cycle in the absence of drugs. Schizonts were collected during both the first and second cycles, DNA was extracted, and Southern hybridizations were performed using DNA probes for apicoplast, mitochondrial, and nuclear genomic sequences. The positions of molecular size markers are indicated.

tribution of all genes, we calculated a histogram of the average underexpression ratio for all unique array features at the hours of peak plastid expression (20 h and 55 h) and plotted the positions of the plastid genes (Fig. 3C). Apicoplast genes were clearly underexpressed relative to other features. Genes carried by the mitochondrion and nuclear genes whose products are targeted to the apicoplast or mitochondrion were unaffected by doxycycline treatment (not shown). Thus, doxycycline treatment specifically disrupts the expression of apicoplast genes.

Replication of apicoplast DNA is disrupted in the progeny of doxycycline-treated parasites. The apicoplast and mitochondrial genomes of *P. falciparum* replicate at the beginning of schizogeny, at the same time as the nuclear genome (27, 32, 43). We compared the replication of nuclear, apicoplast, and mitochondrial genomes in doxycycline-treated and control schizonts. Parasites were incubated with doxycycline during a single cycle, and schizont DNA was extracted and evaluated during this and the subsequent cycle by Southern analysis utilizing probes for the nuclear, apicoplast, and mitochondrial genomes. In the presence of doxycycline, replication of the three genomes was the same as in control schizonts (Fig. 4). In the following cycle, replication of apicoplast DNA, but not nuclear or mitochondrial DNA, was markedly reduced during schizogeny. These results demonstrate that the progeny of doxycycline-treated parasites are unable to replicate the apicoplast genome.

Apicoplast segregation is disrupted in the progeny of doxycycline-treated parasites. We treated *P. falciparum* expressing ACP_I-GFP (40) with doxycycline for a single cycle and then evaluated the morphology of the apicoplasts in trophozoite and schizont stages in this and the subsequent cycle (Fig. 5). In control parasites, the apicoplast elongated into a branched morphology in schizonts before segregating into merozoites, as reported previously (37, 40). In doxycycline-treated parasites, elongation, branching, and segregation of apicoplasts did not appear to be altered. Quantitation by flow cytometry confirmed that the numbers of progeny containing GFP-labeled apicoplasts were the same in doxycycline-treated and control parasites (not shown). The apicoplast was visualized through most of the life cycle in these daughter parasites, indicating that the organelle was intact and that apicoplast-targeting signals were functional. However, as the parasites progressed to schizonts, the elongation, branching, and segregation of apicoplasts were disrupted, and the parasites failed to develop beyond the schizont stage.

To further evaluate the effects of doxycycline on apicoplast and mitochondrial morphologies, we treated parasites stably expressing both ACP_I-DsRed and CS_I-YFP (37) with doxycycline as described above. Both the apicoplast and the mitochondrion displayed typical (10, 30, 37) elongation, branching, and segregation patterns in the presence of doxycycline. In the progeny of doxycycline-treated parasites, the apicoplast was visible, indicating that the organelle was present and that targeting of DsRed was normal, as had been observed for GFP.

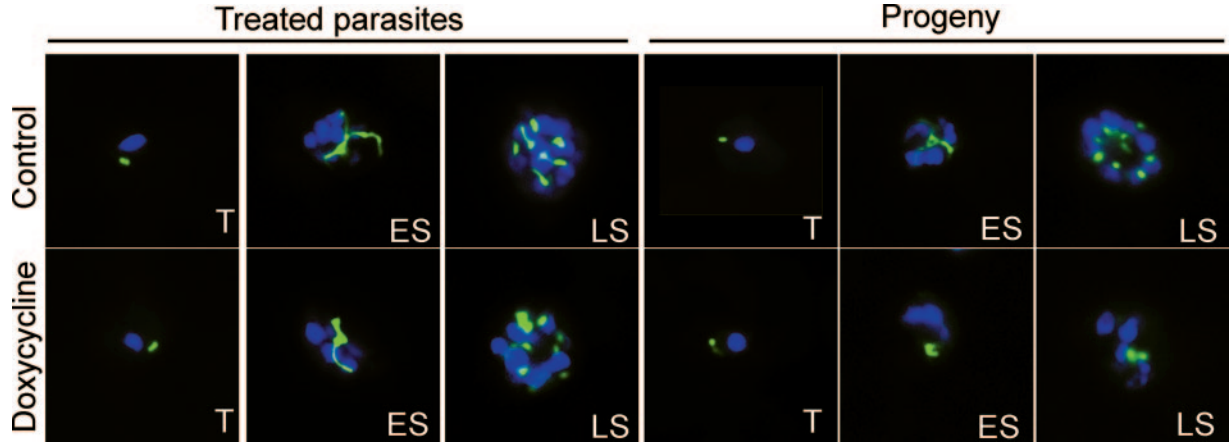

FIG. 5. Development of the apicoplast is blocked in the progeny of doxycycline-treated parasites. Parasites stably expressing the apicoplast-targeted ACP_I-GFP transgene were treated with 1 μM doxycycline or 0.1% DMSO as described in the legend to Fig. 4. Parasites were analyzed by fluorescence microscopy at trophozoite (T), early schizont (ES), and late schizont (LS) stages. The apicoplast appears green; nuclei are stained blue with DAPI.

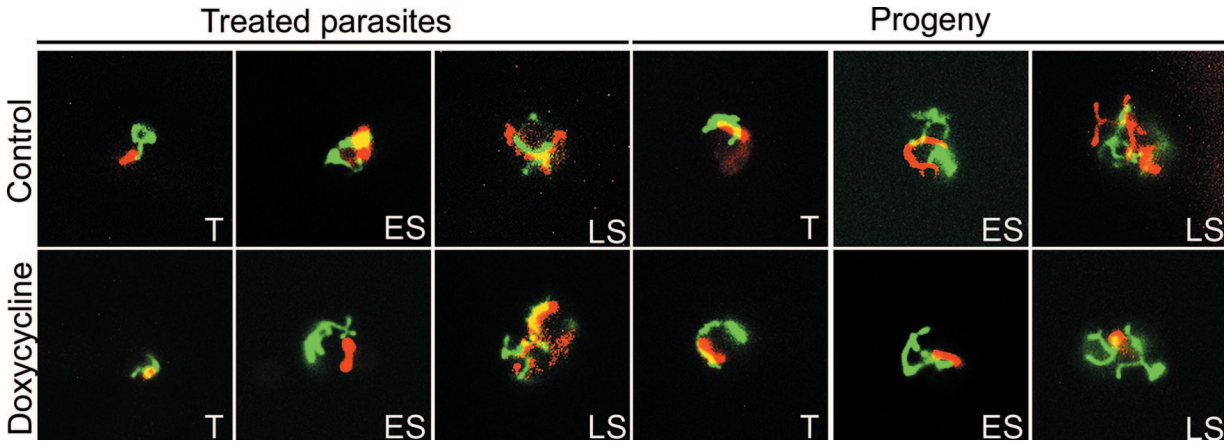

FIG. 6. The mitochondrion elongates and branches normally but is unable to segregate in the progeny of doxycycline-treated parasites. Dually transfected parasites expressing the mitochondrion-targeted CS_1-YFP transgene and the apicoplast-targeted ACP_1-DsRed transgene were treated with 1 μM doxycycline or 0.1% DMSO and analyzed as described in the legend to Fig. 5. Trophozoite (T), early schizont (ES), and late schizont (LS) stages are shown. The mitochondrion appears green, and the apicoplast appears red.

However, apicoplast elongation, branching, and segregation were again disrupted as the parasites initiated schizogeny (Fig. 6). In contrast, the mitochondrion appeared to develop normally, forming elongated and elaborately branched structures in the progeny of doxycycline-treated parasites.

Processing of apicoplast-targeted proteins is disrupted in the progeny of doxycycline-treated parasites. Apicoplast-targeted *P. falciparum* proteins contain a leader sequence that is cleaved upon delivery to the apicoplast (38). We analyzed the processing of apicoplast-targeted GFP by immunoblot analysis with an anti-GFP antibody. Expression and processing of ACP_1-GFP were the same in doxycycline-treated and control parasites during the first cycle. However, processing was blocked in the progeny of doxycycline-treated parasites, but not controls (Fig. 7). The expression and processing of the nuclear-encoded cysteine protease falcipain-3 was unaffected by doxycycline, demonstrating that the inability of parasites to process ACP_1-GFP was due to a specific abnormality in apicoplast function rather than a general defect in protein processing.

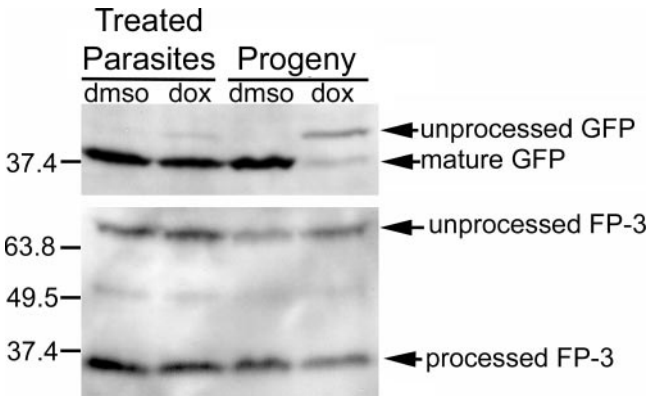

FIG. 7. Apicoplast protein processing is inhibited in the progeny of doxycycline-treated parasites. Proteins from doxycycline-treated and control parasites, treated as described in the legend to Fig. 5, were analyzed by immunoblotting with anti-GFP and anti-falcipain-3 (FP-3) antibodies. The locations of proteins and the positions of molecular mass markers (kDa) are indicated.

DISCUSSION

Tetracyclines are effective antimalarials, but their mechanism of action is unclear. Since these agents block prokaryotic protein synthesis, it has been proposed that they disrupt the mitochondrion or the apicoplast, both of which include prokaryotic ribosomal subunits in their genomes. We have shown that both the mitochondrion and apicoplast appear normal through a cycle of treatment with doxycycline, that these organelles are successfully segregated into daughter parasites, and that they remain intact in the progeny of treated parasites. However, doxycycline specifically blocks the expression of apicoplast genes, leading to the distribution of nonfunctional apicoplasts into daughter parasites and a subsequent block in parasite development. These results indicate that the site of action of tetracyclines is the apicoplast but that loss of apicoplast function is not apparent until late in the cycle following treatment, explaining the slow action of these drugs.

Previous work on the antimalarial effects of tetracyclines demonstrated increased efficacy with prolonged treatment (9, 16, 25). Doxycycline inhibited global protein synthesis only at suprapharmacological concentrations (6), arguing against cytosolic ribosomes as a target for tetracyclines in vivo. Early work examining the mitochondrion as a potential target of tetracyclines demonstrated decreased mitochondrial uptake of rhodamine 123 after 72 h (18). However, this observation may have reflected secondary toxicity to the mitochondrion following primary effects of the drug. Other studies demonstrating depression of mitochondrial enzyme activity (26) and a block in both apicoplast and mitochondrial transcription (22) assessed tetracyclines at concentrations well above those that are clinically achievable.

The slow action of tetracyclines against *P. falciparum* was observed even if trophozoite and early schizont stage parasites were treated for as little as 12 h. Apicoplasts in treated parasites initially appeared morphologically normal, repli-

cated their genomes, processed imported proteins, and segregated into developing merozoites. Doxycycline specifically disrupted the expression of apicoplast genes. However, most of the proteins predicted to be required for apicoplast function are encoded by the nuclear genome (28), so the apicoplast would be expected to perform most functions normally as long as its import machinery remained intact. We propose that, though doxycycline does not prevent apicoplast function initially, the apicoplasts inherited by the progeny of doxycycline-treated parasites contain insufficient levels of apicoplast-encoded proteins required for the importation and processing of the several hundred nuclear genes needed for normal function. This loss of apicoplast function ultimately results in parasite death.

Our data do not support primary action of doxycycline against the mitochondrion, as transcription within this organelle and replication of the mitochondrial genome were not obviously altered over two parasite life cycles. Mitochondria also appeared to segregate normally in the presence of doxycycline, and in the progeny of doxycycline-treated parasites, mitochondria elongated and formed elaborately branched structures similar to those of untreated parasites. We did not observe segregation of these mitochondria at the end of the second cycle, consistent with previous observations that apicoplast segregation always precedes mitochondrial segregation in healthy parasites (37). However, parasites at this stage displayed gross morphological abnormalities, so lack of mitochondrial segregation was likely secondary to loss of apicoplast function.

In addition to data from plasmodia, there is evidence that prokaryotic protein synthesis inhibitors target the apicoplast of the related apicomplexan parasite *Toxoplasma gondii* (7, 13). In *T. gondii*, treatment with clindamycin causes a "delayed-death" phenotype in which progeny are able to invade new host cells but die shortly thereafter. A similar phenotype was observed in *T. gondii* parasites that were unable to inherit an apicoplast due to a genetic-segregation defect, leading to the proposal that the apicoplast is required for the establishment of the parasitophorous vacuole. We have observed that *P. falciparum* parasites containing defective apicoplasts survive until the end of their cycle, arguing against a role in establishing the parasitophorous vacuole. This observation is in agreement with ultrastructural studies on the progeny of clindamycin-treated *T. gondii* parasites, which also contain multiple nuclei and appear unable to complete cell division (7). In both species, death coincides with the initiation of cell division, which occurs early in the *T. gondii* cycle and late in the *P. falciparum* cycle. We propose that the apicoplast is required for the formation of daughter cell plasma membranes, since fatty acid biosynthesis is a likely function of apicoplasts and since our ultrastructural studies indicated that these structures were lacking following doxycycline treatment. Since doxycycline needs to be administered only transiently to disrupt apicoplast function in the following cycle and since parasites containing nonfunctional apicoplasts can survive for nearly 48 h, doxycycline-treated plasmodia are an ideal model system for probing specific functions of the apicoplast.

ACKNOWLEDGMENTS

We thank Geoff McFadden for the ACP_I-GFP and the CS_I-YFP/ACP_I-DsRed transgenic *Plasmodium falciparum* lines, the UCSF Core Cell Imaging Facility for help with electron microscopy, and Julie Lehman, Jamie Koo, Sarah Baxter, and Kevin Lee for excellent technical assistance.

This work was supported by grants from the National Institutes of Health (AI051800 to P.J.R. and AI053862 to J.L.D.), the Medicines for Malaria Venture, the Burroughs Wellcome Fund, and the David and Lucille Packard Foundation. E.L.D. is supported by T32 A1060537. P.J.R. is a Doris Duke Charitable Foundation Distinguished Clinical Scientist.

REFERENCES

1. **Baird, J. K.** 2005. Effectiveness of antimalarial drugs. N. Engl. J. Med. **352:**1565–1577.
2. **Bender, A., G. G. van Dooren, S. A. Ralph, G. I. McFadden, and G. Schneider.** 2003. Properties and prediction of mitochondrial transit peptides from *Plasmodium falciparum*. Mol. Biochem. Parasitol. **132:**59–66.
3. **Bozdech, Z., M. Llinas, B. L. Pulliam, E. D. Wong, J. Zhu, and J. L. DeRisi.** 2003. The transcriptome of the intraerythrocytic developmental cycle of *Plasmodium falciparum*. PLOS Biol. **1:**E5.
4. **Bozdech, Z., J. Zhu, M. P. Joachimiak, F. E. Cohen, B. Pulliam, and J. L. DeRisi.** 2003. Expression profiling of the schizont and trophozoite stages of *Plasmodium falciparum* with a long-oligonucleotide microarray. Genome Biol. **4:**R9.
5. **Bremen, J. G.** 2001. The ears of the hippopotamus: manifestations, determinants, and estimates of the malaria burden. Am. J. Trop. Med. Hyg. **64:**1–11.
6. **Budimulja, A. S., Syafruddin, P. Tapchaisri, P. Wilairat, and S. Marzuki.** 1997. The sensitivity of *Plasmodium* protein synthesis to prokaryotic ribosomal inhibitors. Mol. Biochem. Parasitol. **84:**137–141.
7. **Camps, M., G. Arrizabalaga, and J. Boothroyd.** 2002. An rRNA mutation identifies the apicoplast as the target for clindamycin in *Toxoplasma gondii*. Mol. Microbiol. **43:**1309–1318.
8. **Desjardins, R. E., C. J. Canfield, J. D. Haynes, and J. D. Chulay.** 1979. Quantitative assessment of antimalarial activity in vitro by a semiautomated microdilution technique. Antimicrob. Agents Chemother. **16:**710–718.
9. **Divo, A. A., T. G. Geary, and J. B. Jensen.** 1985. Oxygen- and time-dependent effects of antibiotics and selected mitochondrial inhibitors on *Plasmodium falciparum* in culture. Antimicrob. Agents Chemother. **27:**21–27.
10. **Divo, A. A., T. G. Geary, J. B. Jensen, and H. Ginsburg.** 1985. The mitochondrion of *Plasmodium falciparum* visualized by rhodamine 123 fluorescence. J. Protozool. **32:**442–446.
11. **Eisen, M. B., P. T. Spellman, P. O. Brown, and D. Botstein.** 1998. Cluster analysis and display of genome-wide expression patterns. Proc. Natl. Acad. Sci. USA **95:**14863–14868.
12. **Feagin, J. E., E. Werner, M. J. Gardner, D. H. Williamson, and R. J. Wilson.** 1992. Homologies between the contiguous and fragmented rRNAs of the two *Plasmodium falciparum* extrachromosomal DNAs are limited to core sequences. Nucleic Acids Res. **20:**879–887.
13. **Fichera, M. E., and D. S. Roos.** 1997. A plastid organelle as a drug target in apicomplexan parasites. Nature **390:**407–409.
14. **Foth, B. J., S. A. Ralph, C. J. Tonkin, N. S. Struck, M. Fraunholz, D. S. Roos, A. F. Cowman, and G. I. McFadden.** 2003. Dissecting apicoplast targeting in the malaria parasite *Plasmodium falciparum*. Science **299:**705–708.
15. **Gardner, M. J., N. Hall, E. Fung, O. White, M. Berriman, R. W. Hyman, J. M. Carlton, A. Pain, K. E. Nelson, S. Bowman, I. T. Paulsen, K. James, J. A. Eisen, K. Rutherford, S. L. Salzberg, A. Craig, S. Kyes, M. S. Chan, V. Nene, S. J. Shallom, B. Suh, J. Peterson, S. Angiuoli, M. Pertea, J. Allen, J. Selengut, D. Haft, M. W. Mather, A. B. Vaidya, D. M. Martin, A. H. Fairlamb, M. J. Fraunholz, D. S. Roos, S. A. Ralph, G. I. McFadden, L. M. Cummings, G. M. Subramanian, C. Mungall, J. C. Venter, D. J. Carucci, S. L. Hoffman, C. Newbold, R. W. Davis, C. M. Fraser, and B. Barrell.** 2002. Genome sequence of the human malaria parasite *Plasmodium falciparum*. Nature **419:**498–511.
16. **Geary, T. G., and J. B. Jensen.** 1983. Effects of antibiotics on *Plasmodium falciparum* in vitro. Am. J. Trop. Med. Hyg. **32:**221–225.
17. **Harlow, E., and D. Lane.** 1988. Antibodies: a laboratory manual. Cold Spring Harbor Laboratory, Cold Spring Harbor, N.Y.
18. **Kiatfuengfoo, R., T. Suthiphongchai, P. Prapunwattana, and Y. Yuthavong.** 1989. Mitochondria as the site of action of tetracycline on *Plasmodium falciparum*. Mol. Biochem. Parasitol. **34:**109–115.
19. **Kim, C. C., and S. Falkow.** 2003. Significance analysis of lexical bias in microarray data. BMC Bioinformatics **4:**12.
20. **Kohler, S., C. F. Delwiche, P. W. Denny, L. G. Tilney, P. Webster, R. J. Wilson, J. D. Palmer, and D. S. Roos.** 1997. A plastid of probable green algal origin in apicomplexan parasites. Science **275:**1485–1489.
21. **Lambros, C., and J. P. Vanderberg.** 1979. Synchronization of *Plasmodium falciparum* erythrocytic stages in culture. J. Parasitol. **65:**418–420.

22. **Lin, Q., K. Katakura, and M. Suzuki.** 2002. Inhibition of mitochondrial and plastid activity of *Plasmodium falciparum* by minocycline. FEBS Lett. **515:** 71–74.
23. **O'Rourke, S. M., and I. Herskowitz.** 2002. A third osmosensing branch in *Saccharomyces cerevisiae* requires the Msb2 protein and functions in parallel with the Sho1 branch. Mol. Cell. Biol. **22:**4739–4749.
24. **O'Rourke, S. M., and I. Herskowitz.** 2004. Unique and redundant roles for HOG MAPK pathway components as revealed by whole-genome expression analysis. Mol. Biol. Cell. **15:**532–542.
25. **Pradines, B., C. Rogier, T. Fusai, J. Mosnier, W. Daries, E. Barret, and D. Parzy.** 2001. In vitro activities of antibiotics against *Plasmodium falciparum* are inhibited by iron. Antimicrob. Agents Chemother. **45:**1746–1750.
26. **Prapunwattana, P., W. J. O'Sullivan, and Y. Yuthavong.** 1988. Depression of *Plasmodium falciparum* dihydroorotate dehydrogenase activity in in vitro culture by tetracycline. Mol. Biochem. Parasitol. **27:**119–124.
27. **Preiser, P. R., R. J. Wilson, P. W. Moore, S. McCready, M. A. Hajibagheri, K. J. Blight, M. Strath, and D. H. Williamson.** 1996. Recombination associated with replication of malarial mitochondrial DNA. EMBO J. **15:**684–693.
28. **Ralph, S. A., G. G. Van Dooren, R. F. Waller, M. J. Crawford, M. J. Fraunholz, B. J. Foth, C. J. Tonkin, D. S. Roos, and G. I. McFadden.** 2004. Tropical infectious diseases: metabolic maps and functions of the *Plasmodium falciparum* apicoplast. Nat. Rev. Microbiol. **2:**203–216.
29. **Ryan, E. T., and K. C. Kain.** 2000. Health advice and immunizations for travelers. N. Engl. J. Med. **342:**1716–1725.
30. **Sato, S., K. Rangachari, and R. J. Wilson.** 2003. Targeting GFP to the malarial mitochondrion. Mol. Biochem. Parasitol. **130:**155–158.
31. **Sijwali, P. S., B. R. Shenai, J. Gut, A. Singh, and P. J. Rosenthal.** 2001. Expression and characterization of the *Plasmodium falciparum* haemoglobinase falcipain-3. Biochem. J. **360:**481–489.
32. **Smeijsters, L. J., N. M. Zijlstra, E. de Vries, F. F. Franssen, C. J. Janse, and J. P. Overdulve.** 1994. The effect of (S)-9-(3-hydroxy-2-phosphonylmethoxypropyl) adenine on nuclear and organellar DNA synthesis in erythrocytic schizogony in malaria. Mol. Biochem. Parasitol. **67:**115–124.
33. **Snow, R. W., C. A. Guerra, A. M. Noor, H. Y. Myint, and S. I. Hay.** 2005. The global distribution of clinical episodes of *Plasmodium falciparum* malaria. Nature **434:**214–217.
34. **Thummel, K. E., and D. D. Shen.** 2001. Design and optimization of dosage regimens: pharmacokinetic data, p. 1917–2023. *In* J. G. Hardman, L. E. Limbird, and A. G. Gilman (ed.), Goodman and Gilman's the pharmacological basis of therapeutics, 10th ed. McGraw-Hill, New York, N.Y.
35. **Trager, W., and J. B. Jenson.** 1978. Cultivation of malarial parasites. Nature **273:**621–622.
36. **Vaidya, A. B., and M. W. Mather.** 2005. A post-genomic view of the mitochondrion in malaria parasites. Curr. Top. Microbiol. Immunol. **295:**233–250.
37. **van Dooren, G. G., M. Marti, C. J. Tonkin, L. M. Stimmler, A. F. Cowman, and G. I. McFadden.** 2005. Development of the endoplasmic reticulum, mitochondrion and apicoplast during the asexual life cycle of *Plasmodium falciparum*. Mol. Microbiol. **57:**405–419.
38. **van Dooren, G. G., V. Su, M. C. D'Ombrain, and G. I. McFadden.** 2002. Processing of an apicoplast leader sequence in *Plasmodium falciparum* and the identification of a putative leader cleavage enzyme. J. Biol. Chem. **277:** 23612–23619.
39. **Waller, R. F., P. J. Keeling, R. G. Donald, B. Striepen, E. Handman, N. Lang-Unnasch, A. F. Cowman, G. S. Besra, D. S. Roos, and G. I. McFadden.** 1998. Nuclear-encoded proteins target to the plastid in *Toxoplasma gondii* and *Plasmodium falciparum*. Proc. Natl. Acad. Sci. USA **95:**12352–12357.
40. **Waller, R. F., M. B. Reed, A. F. Cowman, and G. I. McFadden.** 2000. Protein trafficking to the plastid of *Plasmodium falciparum* is via the secretory pathway. EMBO J. **19:**1794–1802.
41. **Walsh, C.** 2003. Antibiotics: actions, origins, resistance. ASM Press, Washington, D.C.
42. **Williamson, D. H., M. J. Gardner, P. Preiser, D. J. Moore, K. Rangachari, and R. J. Wilson.** 1994. The evolutionary origin of the 35 kb circular DNA of *Plasmodium falciparum*: new evidence supports a possible rhodophyte ancestry. Mol. Gen. Genet. **243:**249–252.
43. **Williamson, D. H., P. R. Preiser, P. W. Moore, S. McCready, M. Strath, and R. J. Wilson.** 2002. The plastid DNA of the malaria parasite *Plasmodium falciparum* is replicated by two mechanisms. Mol. Microbiol. **45:**533–542.
44. **Wilson, R. J.** 2005. Parasite plastids: approaching the endgame. Biol Rev. Camb. Philos. Soc. **80:**129–153.
45. **Wilson, R. J., P. W. Denny, P. R. Preiser, K. Rangachari, K. Roberts, A. Roy, A. Whyte, M. Strath, D. J. Moore, P. W. Moore, and D. H. Williamson.** 1996. Complete gene map of the plastid-like DNA of the malaria parasite *Plasmodium falciparum*. J. Mol. Biol. **261:**155–172.